Modeling the Mechanism of Coagulum Formation in Dispersions - Supporting Information

Martin Kroupa, Michal Vonka, and Juraj Kosek*

Department of Chemical Engineering, Institute of Chemical Technology, Prague, Technicka 5, 16628, Prague 6, Czech Republic

E-mail: Juraj.Kosek@vscht.cz

*To whom correspondence should be addressed

A. Structure of the computational domain

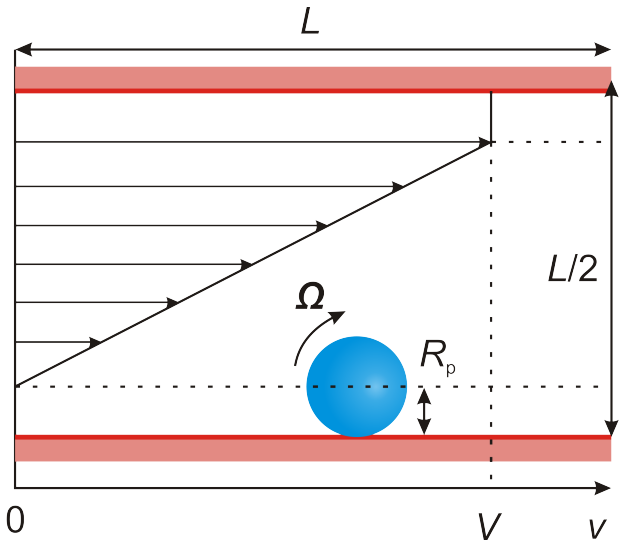

Figure S1: The scheme of the computational domain.

B. Interactions between the particles

DLVO theory

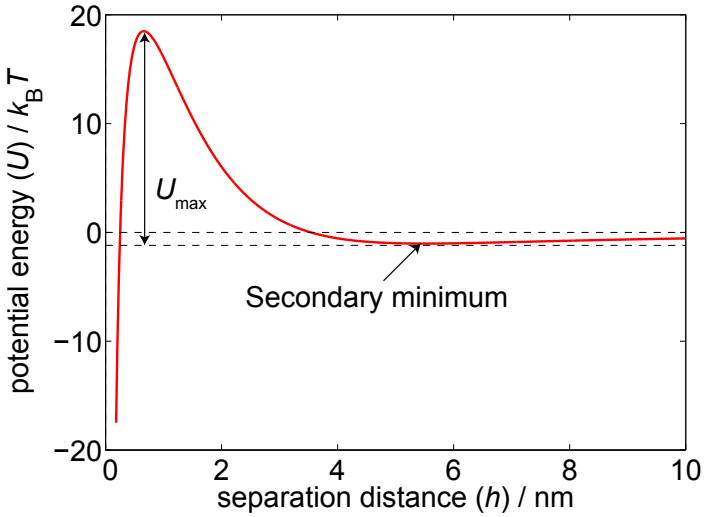

Figure S2: Example of the DLVO potential energy curve for two spheres. Values of parameters are: $R_p = 50\,\text{nm}$, $A_H = 1.3 \times 10^{-20}\,\text{J}$, $\psi_0 = -40\,\text{mV}$, $\kappa^{-1} = 1\,\text{nm}$.

An example of the DLVO potential energy curve is shown in Figure S2. The curve

exhibits typical shape with shallow secondary minimum and potential barrier due to the presence of Electrical Double Layer (EDL). It is clearly the height of this barrier ($U_{\max}$) that is responsible for the stability of the colloidal system.

To provide a better insight into the model, in Figure S3 we demonstrate, how the height of the potential barrier $U_{\max}$ changes with the parameters of the EDL. As expected, the height of the barrier decreases with decreasing absolute value of ψ_0 and increases with increasing κ^{-1}. Both these trends are slightly nonlinear. It is interesting that $U_{\max}$ decreases more steeply with the surface potential for larger particles. It means that larger particles are more sensitive to this parameter than smaller ones and this might be important for practical application.

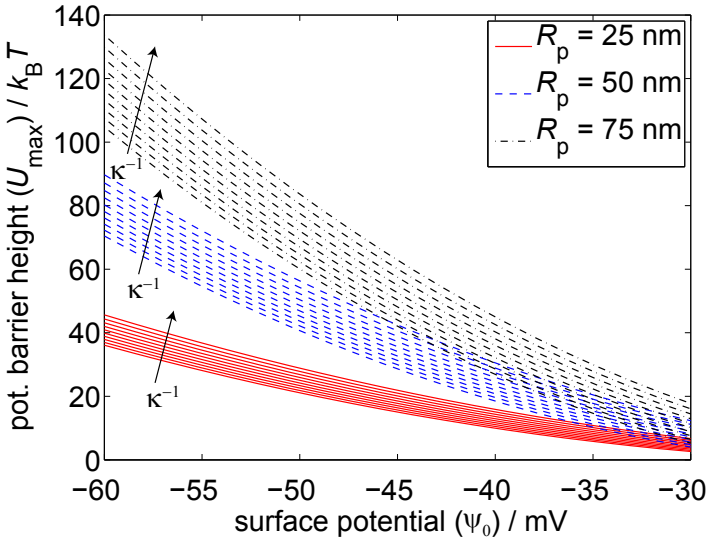

Figure S3: Dependence of the height of the potential barrier ($U_{\max}$) on the surface potential (ψ_0) for different particle radii (R_{p}) and Debye lengths (κ^{-1} from 1 to 2 nm) for interaction of two spheres.

JKR theory

Typical force-distance curve of the JKR theory is shown in Figure S4. When no external force is applied, the particles will stay at the equilibrium point, where the force is zero. As a response to the compressive load, the force between particles becomes repulsive (positive). When teared apart, the particles experience attractive (negative) force until the point, where

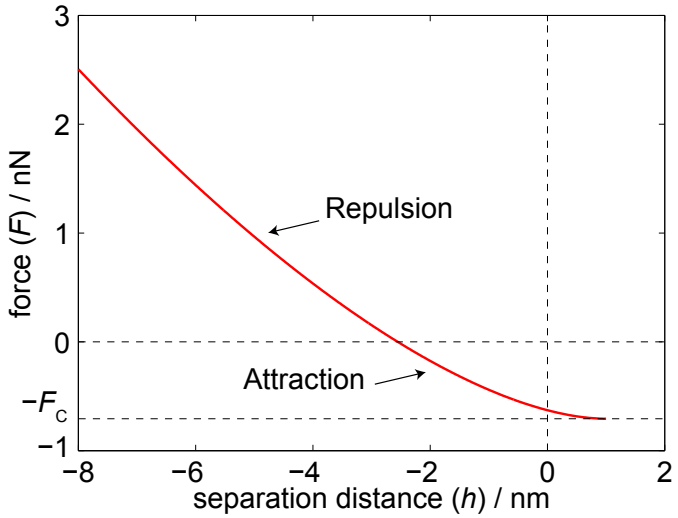

Figure S4: Example of JKR force-distance curve. Values of parameters are: $R_\mathrm{p} = 50\,\mathrm{nm}$, $\gamma = 3\,\mathrm{mN\,m^{-1}}$, $E = 40\,\mathrm{MPa}$, $\nu = 0.2$.

the bond is predicted to break ($h \approx 1\,\mathrm{nm}$). At this point the external force must exceed the maximum adhesion force (F_C) for the bond to be broken.

Tangential interactions

In this section we describe all forces and torques, caused by the interaction of the particle with other particles, which act in the direction tangential to the surface of the particle. There are several different types of the tangential interactions of the particles. Since we restrict ourselves to two spatial dimensions, the twisting of particles is not of a concern, because it involves rotation of the particles in the directions irrelevant for the spatially 2D model. Therefore we provide the formulas for the description of the resistance to sliding and rolling of particles.

The sliding is caused by moving of the surfaces of the touching particles in opposite direction and both rotation and translation can contribute to it. Having the relative velocity ($\mathbf{v}_{ij}^\mathrm{r}$) defined in the section about the dissipative force, we can proceed to the definition of the so-called slip velocity ($\mathbf{v}_{ij}^\mathrm{s}$):

$$\mathbf{v}_{ij}^{\mathrm{s}} = \mathbf{v}_{ij}^{\mathrm{r}} - (\mathbf{v}_{ij}^{\mathrm{r}} \cdot \mathbf{n})\mathbf{n}, \tag{1}$$

where $\cdot$ denotes the dot product of the vectors. Here $\mathbf{v}_{ij}^{\mathrm{s}}$ is the projection of $\mathbf{v}_{ij}^{\mathrm{r}}$ tangent to the particle surface at the contact point. Unit vector in the direction of $\mathbf{v}_{ij}^{\mathrm{s}}$ is given by: $\mathbf{t}_{ij}^{\mathrm{s}} = \frac{\mathbf{v}_{ij}^{\mathrm{s}}}{|\mathbf{v}_{ij}^{\mathrm{s}}|}$.

According to Marshall (2009), the sliding resistance of the particles can be described by the spring-slider model.[1] Unless the sliding force (F_{ij}^{s}) between particles i and j reaches the critical value ($F_{ij}^{\mathrm{s,crit}}$), the sliding is absorbed by the spring. When $|F_{ij}^{\mathrm{s}}| \geq F_{ij}^{\mathrm{s,crit}}$ then the sliding force is limited to the critical value. The critical force $F_{ij}^{\mathrm{s,crit}}$ is obtained from the normal force (F_{ij}^{n}) between particles i and j as follows:

$$F_{ij}^{\mathrm{s,crit}} = \mu_{\mathrm{eff}} |F_{ij}^{\mathrm{n}} + 2F_{\mathrm{C}}|, \tag{2}$$

where μ_{eff} is the effective friction coefficient. In the subcritical case, where $|F_{ij}^{\mathrm{s}}| < F_{ij}^{\mathrm{s,crit}}$, the sliding force is given by:[1]

$$F_{ij}^{\mathrm{s}} = -k_{\mathrm{T}} \left(\int_{t_0}^{t} \mathbf{v}_{ij}^{\mathrm{s}}(\xi) d\xi \right) \cdot \mathbf{t}_{ij}^{\mathrm{s}}, \tag{3}$$

where k_{T} is the tangential stiffness coefficient. The time integral on the right-hand side of Equation 3 describes the tangential elastic displacement from the beginning of the contact at time t_0 to current time t. When the connection between the particles i and j is broken, this integral becomes zero. According to Mindlin (1949), k_{T} can be computed from the following expression:[2]

$$k_{\mathrm{T}} = 8G^{\mathrm{s}} a(t), \tag{4}$$

where $G^{\mathrm{s}} = E/2(1 + \nu_i)$ is the shear modulus of the particles. The corresponding torque ($\mathbf{M}_i^{\mathrm{s}}$) on the particle i caused by the sliding resistance is given by:

$$\mathbf{M}_i^{\mathrm{s}} = R_{\mathrm{p}}^i F_{ij}^{\mathrm{s}} (\mathbf{n} \times \mathbf{t}_{ij}^{\mathrm{s}}). \tag{5}$$

Another type of movement, which has to be taken into account when dealing with rotating particles, is the particle rolling. According to Marshall (2009), rolling is the dominant type of the tangential interaction for colloidal particles, due to their small inertia. For the derivation of rolling resistance we also adopt the spring-slider model as in the case of sliding. We first define the so-called rolling velocity ($\mathbf{v}_{ij}^{\mathrm{L}}$), which is for particles i and j given by[3]:[3]

$$\mathbf{v}_{ij}^{\mathrm{L}} = R(\boldsymbol{\Omega}_i - \boldsymbol{\Omega}_j) \times \mathbf{n}. \tag{6}$$

The direction of rolling ($\mathbf{t}_{ij}^{\mathrm{L}}$) is obtained from:

$$\mathbf{t}_{ij}^{\mathrm{L}} = \frac{\mathbf{v}_{ij}^{\mathrm{L}}}{|\mathbf{v}_{ij}^{\mathrm{L}}|}. \tag{7}$$

Finally the rolling resistance torque ($\mathbf{M}_i^{\mathrm{L}}$) is postulated as[3]:

$$\mathbf{M}_i^{\mathrm{L}} = -k_{\mathrm{L}} \tau^{\mathrm{L}}, \tag{8}$$

where k_{L} is the rolling coefficient and τ^{L} is the rolling displacement obtained from:

$$\tau^{\mathrm{L}} = \left(\int_{t_0}^{t} \mathbf{v}_{ij}^{\mathrm{L}}(\xi) d\xi \right) \cdot \mathbf{t}_{ij}^{\mathrm{L}}, \tag{9}$$

where t_0 and t have the same meaning as in Equation 3. The rolling resistance is caused by the presence of the van der Waals adhesive forces. The expression for k_{L} derived by Dominik and Tielens (1995) is the following:[4]

$$k_{\mathrm{L}} = 4 F_{\mathrm{C}} \left(\frac{a}{a_0} \right)^{\frac{3}{2}}, \tag{10}$$

We refer to the cited papers for further explanation and derivation of the used formulas.

Finally, the model of the rolling resistance is, similarly to the sliding resistance model, created by the connection of spring and slider. The critical rolling displacement ($\tau^{\mathrm{L,crit}}$), which limits the spring, can be computed from:

$$\tau^{\mathrm{L,crit}} = R\theta^{\mathrm{crit}}, \tag{11}$$

where θ^{crit} the critical rolling angle, which is the parameter of the model. If the value of the rolling displacement (τ^{L}) exceeds $\tau^{\mathrm{L,crit}}$, then the critical value is used instead.

The tangential forces and torques are added to the resulting force and torque vectors acting on each particle. The resulting force ($\mathbf{F}_i$) and torque ($\mathbf{M}_i$) acting on particle i (either for the the particle-particle or particle-wall interactions) are obtained as follows:

$$\mathbf{F}_i = F_{\mathrm{N}}\mathbf{n} + F^{\mathrm{s}}\mathbf{t}^{\mathrm{s}}, \tag{12}$$

$$\mathbf{M}_i = R_{\mathrm{p}}F^{\mathrm{s}}(\mathbf{n} \times \mathbf{t}^{\mathrm{s}}) + M^{\mathrm{L}}(\mathbf{t}^{\mathrm{L}} \times \mathbf{n}), \tag{13}$$

where F_{N} is the resulting normal force.

C. Supporting Results

We performed simulations of the system without presence of the EDL on the surface of the particles. Comparison of these results with the prediction from Equation 24 from the main text is shown in Figure S5

It is also interesting to compare the results of the 2D case with the 3D case. We performed preliminary simulations in three spatial dimensions for the system with $\phi = 0.19$ subjected to different shear rates. As can be seen from Figure S6, the 2D and 3D results are in a very good agreement.

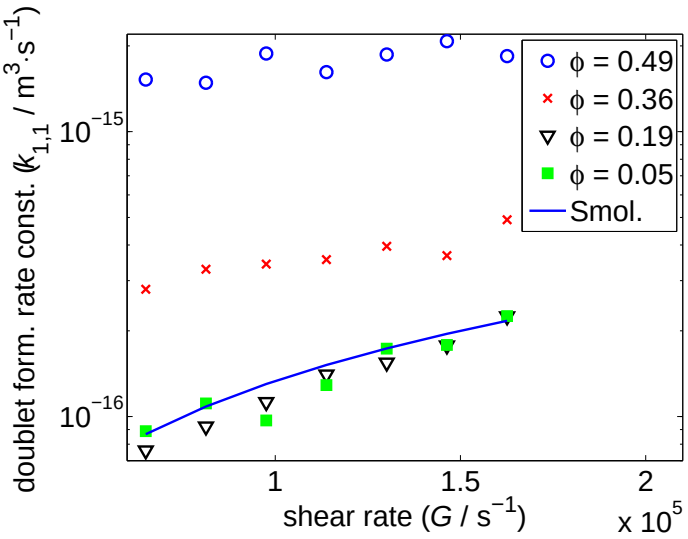

Figure S5: System without the presence of EDL. The rate constant of doublet formation ($k_{1,1}$) as a function of shear rate (G) for different volume fractions of particles (ϕ) compared with the prediction from the Smoluchowski equation (Eq. 24 in the main text).

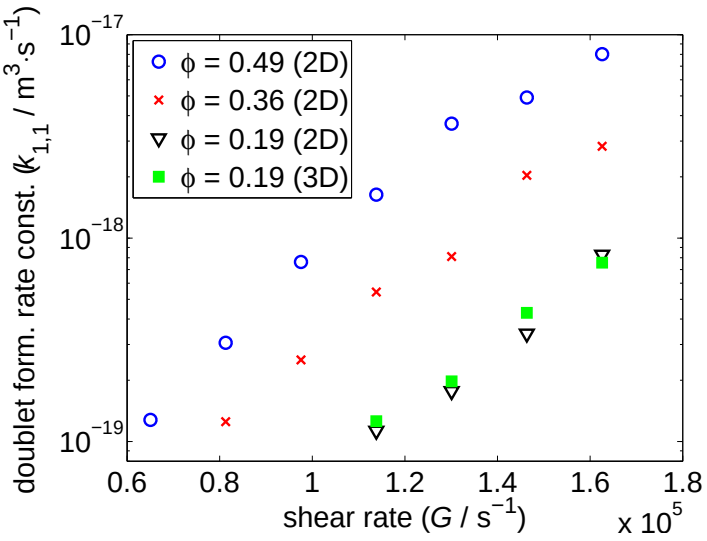

Figure S6: The rate constant of doublet formation ($k_{1,1}$) as a function of shear rate (G) for different volume fractions of particles (ϕ) compared with the 3D simulation.

References

(1) Marshall, J. S. Discrete-element modeling of particulate aerosol flows. *Journal of Computational Physics* **2009**, *228*, 1541–1561.

(2) Mindlin, R. D. Compliance of Elastic Bodies In Contact. *Journal of Applied Mechanics-transactions of the ASME* **1949**, *16*, 259–268.

(3) Marshall, J. S. Particle aggregation and capture by walls in a particulate aerosol channel flow. *Journal of Aerosol Science* **2007**, *38*, 333–351.

(4) Dominik, C.; Tielens, A. G. G. M. Resistance To Rolling In the Adhesive Contact of 2 Elastic Spheres. *Philosophical Magazine A-physics of Condensed Matter Structure Defects and Mechanical Properties* **1995**, *72*, 783–803.